SUPPLEMENTARY METHODS

Human Subjects Recruitment and Ethics Declaration

Hildebrandt Laboratory

The study was approved by the institutional review board (IRB) of Boston Children's Hospital (BCH). We obtained informed consent, clinical data, pedigree information, and blood and/or saliva samples for DNA extraction from subjects who had at least one occurrence of nephrolithiasis or demonstration of nephrocalcinosis on renal ultrasound, manifesting before the age of 25 years. Subjects with a potential secondary cause of NL such as prematurity or use of loop diuretics were excluded from the study.

Khaliq Laboratory

Subjects were recruited during admission for nephrolithiasis, which was confirmed by abdominal ultrasound. The subjects were admitted to one of 5 different tertiary care hospitals in Punjab, Pakistan from July 2014 to December 2016. Subjects received informed consent and provided clinical information (confirmed by their urologist and/or medical records), family history for pedigree construction, and a blood sample for DNA extraction. Consanguinity was determined by history from adult subjects and/or guardians for pediatric cases by asking if parents of subjects were related. Ten subjects did not consent to the study, and 7 subjects were excluded as they had an evident secondary cause of NL (including urinary tract infections and secondary hyperoxaluria). Of the remaining 242 families, adequate DNA samples for genetic studies were obtained in 235. For 31 families, additional family members were recruited upon consent for clinical information and DNA submission, allowing for multi-generational pedigree construction. Serum chemistries, urine metabolites and stone analyses were requested and obtained when available. In total, the cohort consisted of 440 individuals (235 initial probands, 115 additional affected family members and 90

unaffected family members) in 235 families. The study was approved by the institutional review board of Boston Children's Hospital and the Ethical Review Committee for Medical and Biomedical Research, University of Health Sciences, Lahore, Pakistan. It adheres to the Declaration of Helsinki.

Nelson Laboratory

The study was approved by the institutional review board (IRB) of Boston Children's Hospital (BCH). Subjects were recruited from children presenting with a first clinical episode of urolithiasis at the clinic of the Department of Urology at Children's Hospital Boston (Boston MA). Subjects for this study consisted of male and females age 0 years to 21 years presenting with an initial clinical episode of urolithiasis, defined as diagnosis of stone(s) in the kidney or ureter based on imaging studies, or passage of such a stone and verification of stone passage. Subjects completed a comprehensive enrollment interview, including complete medical history of the enrolled subject. DNA samples were collected for genetic studies.

Sayer Laboratory

Patients with kidneys stones were recruited from the regional lithotripsy unit, The Newcastle upon Tyne Hospitals NHS Foundation Trust. Patients gave informed written consent to these studies. Clinical and biochemical data were reviewed. DNA was obtained from patients and relatives where available. The study was approved by the Newcastle upon Tyne Research Ethics Committee (Reference 2003/163).

Halbritter Laboratory

445 study participants with idiopathic NL/NC were enrolled consecutively between June 2016 and October 2018, 276 of which were recruited during admission for NL intervention in the Department of Urology at the University Hospital Leipzig. Study enrollment was based on the clinical diagnosis of

NL/NC. Excluded were subjects with primary hyperparathyroidism and patients with no proof of stone formation upon intervention and imaging. Blood samples were drawn for DNA-extraction after written informed consent. The Medical Ethical Committee of the University of Leipzig (Leipzig, Germany) approved this study (Ethics vote 159/14-ff).

Exome sequencing (ES)

Exome sequencing was performed as previously described[1,2] to discover a novel genetic cause of NL/NC disease using Agilent SureSelect™ human exome capture arrays (Thermo Fisher Scientific) with next generation sequencing (NGS) on an Illumina™ platform. Sequence reads were mapped against the human reference genome (NCBI build 37/hg19) using CLC Genomics Workbench (version 6.5.2) (CLC bio). Genetic location information is according to the February 2009 Human Genome Browser data, hg19 assembly (http://www.genome.ucsc.edu). Downstream processing of aligned BAM files were done using Picard and samtools, and SNV calling was done using GATK5.

High-Throughput Gene Sequencing

We conducted high-throughput variant analysis with a targeted kidney stone gene panel comprising the following known and candidate genes: ADCY10, AGXT, ALPL, AMMECR1, AP2S1, APRT, ATP6V0A4, ATP6V1B1, CA2, CASR, CLCN5, CLCNKB, CLDN10, CLDN16, CLDN19, CYP24A1, FAM20A, GDNF, GNA11, GRHPR, HNF4A, HOGA1, HPRT1, KCNJ1, MAGED2, OCRL, OXGR1, SLC12A1, SLC13A5, SLC22A12, SLC26A1, SLC26A6, SLC26A7, SLC2A9, SLC34A1, SLC34A3, SLC3A1, SLC4A1, SLC7A9, SLC7A13, SLC9A3R1, TRPV5, TRPV6, VDR, and XDH.

Sanger sequencing (ES)

The coding exon of *OXGR1* was amplified by PCR in NL/NC cases using the following primers: Forward 5'-AGGCTGATCTGTTGGTCCTG-3', Reverse 5'-TCATTTGATTCATATTGCCAAAC-3'. These amplified products were sequenced using the Sanger sequencing method. The sequencing data was analyzed using the CLC Genomics Workbench (version 6.5.2) software (CLC Bio, Aarhus, Denmark). The data was aligned to the *OXGR1* reference genome sequence (GRCh37 Chromosome 13: 97,637,973-97,646,984; NM_080818).

Homozygosity Mapping (HM)

For subject B1467_22, the generated VCF file was subsequently used in homozygosity mapper to identify regions of homozygosity based on non-parametric lod (NPL) scores[3]. Genetic regions of homozygosity by descent were plotted across the genome as candidate regions for recessive genes as previously described[4,5].

Variant Calling

Variant calling was performed as previously described[1,2]. Variants within the *OXGR1* locus and/or 30 known NL/NC genes. The variants included were rare in the population with minor allele frequency <1% in dbSNP147. Recessive variants during exome data analysis were included if there were no homozygotes in ExAC and gnomAD databases and minor allele frequency was less than 1%. For dominant variant analysis in the index family B1467, variants were included if there were no homozygotes in ExAC and gnomAD databases and minor allele frequency was less than 0.1%. In subsequent *OXGR1* sequencing in the NL/NC aggregated cohort, variants were filtered with more stringent criteria of no homozygotes and fewer than 5 heterozygotes in ExAC, and no homozygotes

and fewer than 10 heterozygotes in gnomAD. Additionally, variants were non-synonymous and/or located within splice-sites (±6 nucleotides from exon-intron junctions). Subsequently, variant severity was stratified based on protein impact (truncating frameshift or nonsense variants, essential or extended splice-site variants, and missense variants). Splice-site variants were assessed by *in silico* tools MaxEnt and NNSPLICE splice-site variant prediction scores as well as conservation across human splice-sites as described previously[1,2]. Missense variants were assessed based on SIFT, MutationTaster, PolyPhen 2.0 and CADD prediction scores and evolutionary conservation based on manually derived multiple sequence alignments. All remaining variants were confirmed in original subject DNA by Sanger sequencing with segregation in family members when DNA available.

ExAC and gnomAD exome/genome aggregation databases

ExAC and gnomAD databases contain exome and genome data aggregated from worldwide cohorts (60,706 samples and 141,456 samples, respectively)[6,7]. Cohort subjects with pediatric disease and their first/second degree relatives were excluded, although certain biobanks may rarely include such cases at a frequency presumed to be lower than the general population. These databases were employed to assess the frequency of individual variants. Moreover, all *OXGR1* variants in the ExAC cohort were analyzed for deleteriousness as described in the **Variant Calling** section.

Accession numbers

Human OXGR1 full-length protein (GenBank accession NP_001333123), encoded by GenBank accession NM_080818, was presumed as the predominant transcript for this study.

Structural Modeling

Predicted structure for human OXGR1 (AF-Q96P68-F1-model_v2) was downloaded from AlphaFold[8]. PyMOL was employed to visualize and mutagenize amino acids altered by human *OXGR1* variants,

and neighboring amino acid residues within 4 angstroms were identified. Site Directed Mutator was used to predict biophysical impact of variants on protein stability[9].

Single-cell mRNA sequencing data analysis

Heatmap results depicting differential mRNA expression levels (from z-scores) was based on single-cell transcriptomics data from seven healthy 4-8 week old C57BL/6 male mice[10]. Processed data from each set was queried for percent expression in defined cell clusters. Queried data was normalized using z-score calculation as described[10].

cDNA cloning

cDNA clones were purchased from the following sources: human *OXGR1 (Harvard PlasmID Database*, HsCD00369784). Mutagenesis was performed using the QuikChange II XL Site-Directed Mutagenesis Kit (Agilent Technologies). Expression constructs (pRK5-N-Myc) were produced using LR Clonase (Invitrogen, Thermo Fisher Scientific) following the manufacturer's instructions.

Eukaryotic Cell lines

The experiments described here were performed using HEK293T cell. HEK293T cells were purchased from the ATCC Biological Resource Center.

Antibodies, reagents, quantitative PCR reagents

The following primary antibodies were used: rabbit anti-OXGR1 (Novus Biologicals, NBP2-42169), mouse anti-myc (Santa Cruz, SC-40), mouse HRP-linked anti-beta actin (Abcam, ab20272). HRP-labeled secondary antibodies were purchased from Santa Cruz Biotechnology.

Xenopus oocyte reagents

$^{45}CaCl_2$ was from PerkinElmer (Waltham, MA). Restriction enzymes and T4 DNA ligase were from New England Biolabs (Beverly, MA). EXPAND High-fidelity PCR System was from Roche (Indianapolis, IN). Other reagent-grade chemicals were from Sigma-Aldrich (St. Louis, MO) or Fluka (Milwaukee, WI).

Xenopus oocyte solutions

MBS consisted of (in mM) 88 NaCl, 1 KCl, 2.4 $NaHCO_3$, 0.82 $MgSO_4$, 0.33 $Ca(NO_3)_2$, 0.41 $CaCl_2$, and 10 HEPES (pH 7.4). ND-96 consisted of (in mM) 96 NaCl, 2 KCl, 1.8 $CaCl_2$, 1 $MgCl_2$, and 5 Na HEPES (pH 7.4). For flux experiments conducted at pH 5.0, Na HEPES was replaced by equimolar MES. NMDG-97 consisted of (in mM) 97.3 N-Methyl-D-glucamine, 2.03 KCl, 1.2 $CaCl_2$, 1 $MgCl_2$, and 5 Na HEPES (pH 7.4). Cl^- substitution was achieved by equimolar replacement with cyclamate. Cl^- salts of K^+, Ca^{2+}, and Mg^{2+} were substituted by the corresponding equimolar gluconate salts as necessary.

cRNA synthesis and expression in *Xenopus* oocytes

Capped cRNA was transcribed at 37^{o}C from linearized OXGR1 cDNA template using the Megascript T7 kit (Life Technologies), purified with the RNeasy mini-kit (Qiagen, Valencia, CA), and quantitated by Nanodrop spectrometer (ThermoFisher, Waltham, MA). RNA integrity was verified by formaldehyde gel electrophoresis. Mature female *Xenopus laevis* (Dept. Systems Biology, Harvard Med. School or NASCO, Fort Atkinson, WI) were subjected to partial ovariectomy under hypothermic tricaine anesthesia following protocols approved by the Institutional Animal Care and Use Committee of Beth Israel Deaconess Med. Ctr. Stage VI oocytes were prepared by overnight incubation of ovarian fragments in MBS with 2 mg/ml collagenase B (Alfa Aesar, Ward Hills, MA), followed by a 20

min rinse in Ca^{2+}-free MBS, with subsequent manual selection and defolliculation as needed. Oocytes were injected with cRNA on the day of isolation, and maintained at 17.5°C in MBS supplemented with gentamicin (10 µg/mL) for 72 h.

Isotopic influx experiments:

Unidirectional $^{45}Ca^{2+}$ influx into individual oocytes was carried out for 30 min in 148 µL NMDG-97 and 2 µL $^{45}CaCl_2$ (~2 µCi; final bath [Ca^{2+}] 1.8 mM). Influx experiments were terminated with three washes of oocytes in ice-cold isotonic NMDG chloride solution. Washed oocytes were individually lysed in 150 µL 2% sodium dodecyl sulfate (SDS). Triplicate 10 µL aliquots of influx bath solution were used to calculate specific activity of radiolabeled substrate ions. Oocyte ion uptakes were calculated from cpm values of cold-washed oocytes and from bath specific activity.

Confocal immunofluorescence microscopy:

Oocytes were injected with 50 ng human MYC-tagged OXGR1 cRNA. cRNA-injected oocytes and uninjected oocytes were incubated 72h at 17.5°C in MBS containing gentamicin (10 µg/mL). 10 oocytes in each experimental group were fixed in 3% paraformaldehyde (PFA) in phosphate-buffered saline (PBS) for 30 min at room temperature, washed 3 times with PBST, permeablized with 1% SDS in PBS supplemented with 0.02% Na azide (PBS-azide) for 1 to 2 minutes, and washed again 3 times with PBST.

Fixed, permeabilized oocytes were incubated overnight at 4°C in 0.5 ml PBST containing affinity-purified polyclonal rabbit anti-Myc Ig (Cell Signaling #71D10) at 1:1000 dilution, rinsed in PBST, followed by Cy3-conjugated donkey-anti-rabbit secondary Ig (Cell Signaling) for 90 min at 20°C. Stained oocytes were washed 3x in PBST, 2x in PBS-azide and post-fixed in PFA for 10 minutes. Fixed oocytes were washed 2x in PBST, extensively washed with PBS-azide, and stored in

PBS-azide at 4°C until imaged. Cy3-labeled oocytes aligned in uniform orientation along a plexiglass groove were sequentially imaged through the 10x objective of a Zeiss LSM510 laser scanning confocal microscope, using the 543 nm laser line at 512 x 512 resolution at a uniform setting of 80% intensity, pinhole 54 (1.0 Airy units), detector gain 650, Amp gain 1, zero amp offset.

Polypeptide abundance at or near the oocyte surface was estimated by quantitation of specific fluorescence intensity (FI) at the circumference of one quadrant of an equatorial focal plane image of the oocyte (Image J v. 1.38, National Institutes of Health). Background correction was performed by subtraction from the FI of each cRNA-injected oocyte the mean FI value of a comparable circumference area from an equatorial plane quadrant of water-injected oocytes.

Oocyte lysate immunoblots:

20 oocytes injected with OXGR1 cRNA (50 ng) were placed in 1.5 mL MBS and incubated 72 h at 17.5°C. MBS was then aspirated and replaced with RIPA buffer containing Complete Protease inhibitor (6 µl per oocyte), vortexed vigorously and immediately frozen at -80°C for $\geq$2 hours. The subsequently thawed mixture was again vortexed, then centrifuged 20-30 minutes at 4°C at maximal microfuge speed. The opalescent infranatant separating pellet and the foamy supranatant was withdrawn and subjected to two more cycles of vortexing, 4°C centrifugation, and infranatant harvest. The final, clarified protein extracts were assayed for protein content by the BCA method and stored at -80°C until use. 20 µg of extract protein was brought to 10 µl volume with RIPA buffer containing protease inhibitors, and 4 µl SDS load buffer containing β-mercaptoethanol was added. The sample mixture was incubated at room tempterature for 30 min, then loaded on an 8-16% polyacrylamide gradient tris-glycine gel (BIO-RAD) and subjected to SDS-PAGE. Protein was transferred to PVDF membrane (BioRad TurboBlot), washed in TBST, and blocked 1 hr with TBST plus 5% powdered milk. The blocked membrane was washed with TBST and incubated overnight at 4°C with affinity

purified rabbit polyclonal anti-Myc Ig (Cell Signaling #71D10) diluted 1:500 in TBST/5% BSA, then further washed and incubated 1 hr with horseradish peroxidase-coupled goat anti-rabbit Ig (Thermo Scientific #31460) diluted 1:8000 in TBST/5% milk. The peroxidase signal was developed (Supersignal West DURA kit, Life Technologies), imaged (FluorChem E, Bio-Techne), and quantitated by densitometry (Image J).

Statistics:

Data reported as means ± SE (ion flux, ion current, fluorescence intensity) were compared by Student's paired or unpaired two-tailed t tests (Microsoft Excel), or by ANOVA with Tukey post-hoc analysis (SigmaPlot). $P < 0.05$ was interpreted as statistically significant.

Statistics

Graphpad Prism 8.0.0 software or SigmaPlot software was used to perform statistical testing.

Web Resources

UCSC Genome Browser, genome.ucsc.edu

Ensembl Genome Browser, www.ensembl.org

ExAC and gnomAD browsers, gnomad.broadinstitute.org

Polyphen2, genetics.bwh.harvard.edu/pph2

Sorting Intolerant From Tolerant (SIFT), sift.jcvi.org

MutationTaster, www.mutationtaster.org

Combined Annotation Dependent Depletion, https://cadd.gs.washington.edu/

SMART, smart.embl-heidelberg.de

Protein Data Bank, www.rcsb.org

GPCR Sarfari, ebi.ac.uk/chembl/sarfari/gpcrsarfari

METHODS REFERENCES

1. Connaughton, D. M. *et al.* Monogenic causes of chronic kidney disease in adults. *Kidney International* **95**, 914–928 (2019).
2. Braun, D. A. *et al.* Mutations in multiple components of the nuclear pore complex cause nephrotic syndrome. *J Clin Invest* **128**, 4313–4328 (2018).
3. Seelow, D., Schuelke, M., Hildebrandt, F. & Nürnberg, P. HomozygosityMapper—an interactive approach to homozygosity mapping. *Nucleic Acids Research* **37**, W593–W599 (2009).
4. Hildebrandt, F. *et al.* A Systematic Approach to Mapping Recessive Disease Genes in Individuals from Outbred Populations. *PLOS Genetics* **5**, e1000353 (2009).
5. Sayer, J. A. *et al.* The centrosomal protein nephrocystin-6 is mutated in Joubert syndrome and activates transcription factor ATF4. *Nature Genetics* **38**, 674 (2006).
6. Lek, M. *et al.* Analysis of protein-coding genetic variation in 60,706 humans. *Nature* **536**, 285–291 (2016).
7. Karczewski, K. J. *et al.* The mutational constraint spectrum quantified from variation in 141,456 humans. *Nature* **581**, 434–443 (2020).
8. Jumper, J. *et al.* Highly accurate protein structure prediction with AlphaFold. *Nature* **596**, 583–589 (2021).
9. Ochoa-Montaño, B., Pandurangan, A. P., Blundell, T. L. & Ascher, D. B. SDM: a server for predicting effects of mutations on protein stability. *Nucleic Acids Research* **45**, W229–W235 (2017).
10. Park, J. *et al.* Single-cell transcriptomics of the mouse kidney reveals potential cellular targets of kidney disease. *Science* **360**, 758 (2018).

Supplementary Table 1. Clinical Phenotypes of *OXGR1* variant-associated NL/NC families

Family_ Individual	NL (Y/N)	Recurrent NL (Y/N)	Stone Composition	NC (Y/N)	Age of Onset (yrs)	NL/NC Fam Hx (Y/N)	Serum Electrolytes Renal Function Blood Gas Endocrine Labs	Urinary Studies	Management
Css1201	Y	Y	CaOx	N	14	ND	BUN 4.2 mmol/L (NORM) Cr 104 umol/L (NORM) Na 137 mmol/L (NORM) K 4.4 mmol/L (NORM)	Ca 0.19 mmol/mmol Cr (NORM) Na 408 mmol/day (HIGH)	ND
URO 146_21	Y	Y	ND	N	65	Y	ND	ND	Ureteroscopy for NL removal
URO 146_11	Y	Y	ND	N	27	Y	ND	ND	ND
B1467_22	Y	Y	CaOx Mono	Y	6	Y	BUN 21 mg/dL (HIGH) Cr 0.9 mg/dL (HIGH) Na 139 mmol/L (NORM) K 3.5 mmol/L (NORM) HCO3 19 mmol/L (LOW) Ca 8.5 mg/dL (NORM) PO 5.5 mg/dL (NORM) UrAc 6 mg/dL (NORM) Venous pH 7.32 (NORM) Venous pCO2 35 (LOW)	Spec Grav 1.015 Urine pH 6,5 Urine Ca 1.15 mg/kg/day (NORM) Urine Ox 50 mg/24hr/1.73 (HIGH) Urine Mg 91.8 mg/24hr/1.73 (NORM) Urine Citrate 373 mg/g Cr (LOW) Urine UrAc 506 mg/24hr/1.73 (NORM) Urine Ca-Oxalate Crystalluria	Hydration, Citrate.
B1467_21	N	NA	NA	Y	ND	Y	BUN 19 mg/dL (HIGH) Cr 0.7 mg/dL (HIGH) Na 136 mEq/L (NORM) K 3.8 mEq/L (NORM) Cl 99 mEq/L (NORM) HCO3 21 mEq/L (NORM) Ca 9.8 mg/dL (NORM) Mg 1.9 mg/dL (NORM) PO 5.4 mg/dL (NORM) UrAc 5.5 mg/dL (NORM) Venous pH 7.32 (NORM) Venous pCO2 38 (LOW)	Spec Grav 1.010 Urine pH 6.4 Urine Ca 1.2 mg/kg/day (NORM) Urine Ox 65 mg/24hr/1.73 (HIGH) Urine Mg 92 mg/24hr/1.73 (NORM) Urine Citrate 380 mg/g Cr (LOW) Urine UrAc 500 mg/24hr/1.73 (NORM) Urine Ca-Oxalate Crystalluria	ND
B1467_23	N	NA	NA	Y	ND	Y	BUN 10 mg/dL (NORM) Cr 0.6 mg/dL (NORM) Na 138 mEq/L (NORM) K 4 mEq/L (NORM) Cl 100 mEq/L (NORM) HCO3 19 mEq/L (LOW) Ca 10.5 mg/dL (NORM) Mg 2 mg/dL (NORM) PO 5.2 mg/dL (NORM) UrAc 5.4 mg/dL (NORM) Venous pH 7.38 (NORM) Venous pCO2 40 (LOW)	Spec Grav 1.015 Urine pH 6.3 Urine Ca 1.15 mg/kg/day (NORM) Urine Ox 60 mg/24hr/1.73 (HIGH) Urine Mg 97 mg/24hr/1.73 (NORM) Urine Citrate 385 mg/g Cr (LOW) Urine UrAc 480 mg/24hr/1.73 (NORM) Urine Ca-Oxalate Crystalluria	ND
B1467_24	N	NA	NA	Y	ND	Y	BUN 12 mg/dL (NORM) Cr 0.5 mg/dL (NORM) Na 138 mEq/L (NORM) K 3.5 mEq/L (NORM) Cl 101 mEq/L (NORM) HCO3 20 mEq/L (NORM) Ca 9.5 mg/dL (NORM)	Spec Grav 1.020 Urine pH 6.6 Urine Ca 1.20 mg/kg/day (NORM) Urine Ox 66 mg/24hr/1.73 (HIGH) Urine Mg 90 mg/24hr/1.73 (NORM) Urine Citrate 388 mg/g Cr (LOW) Urine UrAc 505 mg/24hr/1.73 (NORM)	ND

							Mg 1.9 mg/dL (NORM) PO 5.2 mg/dL (NORM) UrAc 4.5 mg/dL (NORM) Venous pH 7.32 (NORM) Venous pCO2 35 (LOW)	Urine Ca-Oxalate Crystalluria	
B1467_12	N	NA	NA	Y	ND	Y	ND	ND	ND
B641_MA1009	Y	Y	51% CaOx Mono 45% CaOx Di	N	16	ND	BUN 9 mg/dL (NORM) Cr 0.6 mg/dL (NORM) Na 140 mEq/L (NORM) K 4.15 mEq/L (NORM) Cl 102 mEq/L (NORM) HCO3 27 mEq/L (NORM) Ca 10.4 mg/dL (NORM) Mg 2.0 mg/dL (NORM) PO 4.1 mg/dL (NORM) UrAc 3.6 mg/dL (NORM) PTH 14.8 pg/mL (NORM) 25-OH VitD 21.5 ng/mL (NORM) 1,25-OH VitD 76 pg/mL (NORM)	pH 6.761 Ca/24hr 133 mg (NORM) Ca/kg/24hr 2.7 mg/kg (NORM) CaOx SS 9.21 (NORM) CaPh SS 2.57 (HIGH) Ox/24hr 49 (HIGH) Na/24hr 239 (HIGH) UrAc/24hr 0.553 (NORM) UrAc SS 0.19 (NORM)	ESWL, Hydration.
JAS-F68_21	Y	Y	CaOx	Y	50	Y	BUN 5.2 mmol/L (NORM) Cr 81 umol/L (NORM) Na 137 mEq/L (NORM) K 3.93 mEq/L (NORM) Ca 2.36 mg/dL (NORM) Ionized Ca 1.15 mmol/L (LOW) PO 1.11 mmol/L (NORM)	Ca 0.61 mmol/mmol Cr (NORM, ULN 0.7 mmol/mmol)	ESWL (twice), PCNL (3 times).
B431_21	Y	N	95% CaOx Mono 5% CaPO	N	18	Y	BUN 8 mg/dL (NORM) Cr 0.5 mg/dL (NORM) Na 137 mEq/L (NORM) K 3.93 mEq/L (NORM) Cl 102 mEq/L (NORM) HCO3 23 mEq/L (NORM) Ca 9.7 mg/dL (NORM) Mg 2.1 mg/dL (NORM) PO 3.4 mg/dL (NORM) UrAc 4.2 mg/dL (NORM) PTH 46.5 pg/mL (NORM) 25-OH VitD 11.6 ng/mL (LOW) 1,25-OH VitD 74 pg/mL (NORM)	Spec Grav 1.011 pH 6.5 Ca 0.14 g/g Cr (NORM) Ox <0.01 g/g Cr (NORM) Mg 0.07 g/g Cr (NORM) Citrate 769 mg/g Cr (NORM) UrAc 0.55 g/g Cr (NORM) No crystalluria	Ureteroscopy and Basket Extraction of unilateral NL.

Abbreviations: 1,25-OH VitD, 1,25-dihydroxy Vitamin D; 24hr, 24 hours; 25-OH VitD, 25-hydroxy Vitamin D; BUN, blood urea nitrogen; Ca, calcium; CaOx, calcium oxalate; CaPO, calcium phosphate; Cl, chloride; Cr, creatinine; Di, dihydrate; ESWL, Extracorporeal Shock Wave Lithotripsy; Fam Hx, family history; HCO3, bicarbonate; K, potassium; Mg, magnesium; Mono, monohydrate; N, no; Na, sodium; NA, not applicable; NC, nephrocalcinosis; ND, no data; NL, nephrolithiasis; NORM, normal; Ox, oxalate; PCNL, Percutaneous Nephrolithonomy; PO, phosphorous; PTH, parathyroid hormone; SS, supersaturation; UrAc, uric acid; Y, yes; yrs, years.

Supplementary Table S2. Variants of unknown significance in Family B1467

Family_ Individual	Sex	Gene Symbol	Genotype	Nucleotide Change	AA Change	*In silico* Severity Scores	Conservation Through	ExAC; gnomAD (H, h, Tot)
B1476 _21 _22 _23 _24 _12 _11	 F F M M F M	*LMX1B*	 HET HET HET HET HET WT	c.650G>A	p.Arg217Gln	SIFT DL MT DC PP2 PSD CADD 26.6	*D. melanogaster*	NP 0/4/275398
B1476 _21 _22 _23 _24 _12 _11	 F F M M F M	*GAS6*	 HET HOM HET WT HET HET	c.460G>C	p.Asp154His	SIFT DL MT DC PP2 PD CADD 23.9	*G. gallus*	0/29/120644 0/85/282404

Abbreviations: AA, amino acid; CADD, Combined Annotation Dependent Depletion; DC, disease causing; DL, deleterious; ExAC, Exome Aggregation Consortium; F, female; gnomAD Genome Aggregation database; H, homozygous individuals in database; h, heterozygous alleles of particular variant in database; HET, heterozygous genotype; HOM, homozygous genotype; M, male; NP, not present in variant database; PD, probably disease causing; PP2, PolyPhen-2 prediction score; PSD, possibly disease causing; SIFT, Sorting Tolerant From Intolerant prediction score; Tot, total alleles at position in database; WT, wildtype genotype.

Supplementary Table S3. Heterozygous variant of unknown significance (VUS) in the gene *OXGR1* (NM_080818) in 1 family with nephrolithiasis.

Family_ Individual	Nucleotide Change	AA Change	*In silico* Severity Scores	ACMG/AMP Classification (Criteria)	Conser-vation	ExAC; gnomAD (H, h, Tot)	SEX	Country of Origin / Ethnicity	Age of onset (yrs)	Stone Disease
B431_21	c.860C>T	p.Ser287Phe	PP2 PD SIFT DL CADD 5.6	VUS (PM2, PP3, BS3)	*D. rerio*	NP NP	F	Bosnia	18	CaOx NL

Abbreviations: AA, amino acid; CADD, Combined Annotation Dependent Depletion; CaOx, calcium oxalate; DL, deleterious; ExAC, Exome Aggregation Consortium; F, female; gnomAD Genome Aggregation database; H, homozygous individuals in database; h, heterozygous alleles of particular variant in database; het, heterozygous; NL nephrolithiasis; NP, not present in variant database; PD, probably damaging; PP2, PolyPhen-2 prediction score; Seg, segregation; SIFT, Sorting Tolerant From Intolerant prediction score; Tot, total alleles at position in database; VUS, variant of unknown significance; yrs, years.

Table S4. Deleterious Rare *OXGR1* Variants in ExAC exome database

Chromosome	Position	Reference	Alternate	Transcript Consequence	Protein Consequence	SIFT Call	PP	PHRED	Allele Count	Homozygote Count
13	97640013	T	C	c.1A>G	p.Met1?	DAMAGING	benign	21.8	1	0
13	97640011	C	A	c.3G>T	p.Met1?	DAMAGING	benign	22.1	1	0
13	97639985	T	A	c.29A>T	p.Asn10Ile	DAMAGING	possibly_damaging	22.3	1	0
13	97639977	C	A	c.37G>T	p.Asp13Tyr	DAMAGING	benign	21	3	0
13	97639963	A	T	c.51T>A	p.Tyr17Ter	DAMAGING	NA	28	1	0
13	97639910	T	C	c.104A>G	p.Tyr35Cys	DAMAGING	probably_damaging	25.3	2	0
13	97639845	T	C	c.169A>G	p.Thr57Ala	DAMAGING	benign	22.3	1	0
13	97639841	T	C	c.173A>G	p.Tyr58Cys	DAMAGING	probably_damaging	24.2	1	0
13	97639815	T	C	c.199A>G	p.Ser67Gly	DAMAGING	benign	20.5	1	0
13	97639812	T	C	c.202A>G	p.Ser68Gly	DAMAGING	probably_damaging	25.7	1	0
13	97639811	C	T	c.203G>A	p.Ser68Asn	DAMAGING	probably_damaging	25.3	1	0
13	97639796	A	T	c.218T>A	p.Leu73Gln	DAMAGING	possibly_damaging	26.3	1	0
13	97639791	G	C	c.223C>G	p.Leu75Val	DAMAGING	probably_damaging	23.3	2	0
13	97639779	C	A	c.235G>T	p.Asp79Tyr	DAMAGING	probably_damaging	28	1	0
13	97639779	C	T	c.235G>A	p.Asp79Asn	DAMAGING	probably_damaging	28.1	1	0
13	97639755	G	C	c.259C>G	p.Pro87Ala	DAMAGING	probably_damaging	25.3	2	0
13	97639754	G	T	c.260C>A	p.Pro87His	DAMAGING	probably_damaging	26.8	2	0
13	97639743	G	A	c.271C>T	p.His91Tyr	DAMAGING	benign	20.8	1	0
13	97639742	T	C	c.272A>G	p.His91Arg	DAMAGING	probably_damaging	24.2	1	0
13	97639737	A	G	c.277T>C	p.Tyr93His	DAMAGING	probably_damaging	24.6	1	0
13	97639735	A	T	c.279T>A	p.Tyr93Ter	DAMAGING	NA	23.5	1	0
13	97639725	C	T	c.289G>A	p.Glu97Lys	DAMAGING	benign	20.6	4	0
13	97639717	C	A	c.297G>T	p.Trp99Cys	DAMAGING	probably_damaging	31	1	0
13	97639709	C	T	c.305G>A	p.Gly102Glu	DAMAGING	probably_damaging	27.4	2	0
13	97639701	T	C	c.313A>G	p.Met105Val	DAMAGING	benign	22.5	1	0
13	97639700	A	G	c.314T>C	p.Met105Thr	DAMAGING	possibly_damaging	25.5	1	0
13	97639685	C	T	c.329G>A	p.Arg110His	DAMAGING	benign	21.6	1	0
13	97639647	A	C	c.367T>G	p.Phe123Val	DAMAGING	probably_damaging	26.4	1	0
13	97639643	A	C	c.371T>G	p.Leu124Arg	DAMAGING	probably_damaging	27.9	1	0
13	97639640	G	A	c.374C>T	p.Thr125Ile	DAMAGING	probably_damaging	26	2	0
13	97639622	C	G	c.392G>C	p.Arg131Pro	DAMAGING	probably_damaging	29.8	1	0
13	97639598	AT	A	c.415delA	p.Met139Ter	#N/A	#N/A	#N/A	2	0
13	97639595	C	T	c.419G>A	p.Ser140Asn	DAMAGING	benign	22.3	3	0
13	97639554	A	C	c.460T>G	p.Cys154Gly	DAMAGING	probably_damaging	25.5	3	0
13	97639529	A	G	c.485T>C	p.Leu162Pro	DAMAGING	probably_damaging	27.2	1	0
13	97639511	A	G	c.503T>C	p.Met168Thr	DAMAGING	benign	23.3	2	0
13	97639459	G	T	c.555C>A	p.Asp185Glu	DAMAGING	possibly_damaging	23.1	1	0
13	97639457	A	G	c.557T>C	p.Leu186Pro	DAMAGING	probably_damaging	28.4	1	0
13	97639443	C	A	c.571G>T	p.Glu191Ter	DAMAGING	NA	37	1	0
13	97639429	A	C	c.585T>G	p.Ile195Met	DAMAGING	possibly_damaging	23.5	1	0
13	97639420	G	C	c.594C>G	p.Tyr198Ter	DAMAGING	NA	36	1	0
13	97639408	CA	C	c.605delT	p.Leu202Ter	#N/A	#N/A	#N/A	1	0
13	97639341	G	C	c.673C>G	p.Leu225Val	DAMAGING	probably_damaging	18.95	1	0
13	97639317	T	G	c.697A>C	p.Ser233Arg	DAMAGING	benign	21.5	3	0
13	97639292	C	T	c.722G>A	p.Arg241Lys	DAMAGING	probably_damaging	22.8	1	0
13	97639259	A	T	c.755T>A	p.Val252Glu	DAMAGING	possibly_damaging	23.7	1	0
13	97639259	A	C	c.755T>G	p.Val252Gly	DAMAGING	possibly_damaging	23.4	1	0
13	97639256	C	T	c.758G>A	p.Cys253Tyr	DAMAGING	probably_damaging	26.3	1	0
13	97639248	G	A	c.766C>T	p.Pro256Ser	DAMAGING	probably_damaging	25.1	1	0
13	97639224	G	A	c.790C>T	p.Arg264Trp	DAMAGING	possibly_damaging	24	2	0
13	97639223	C	T	c.791G>A	p.Arg264Gln	DAMAGING	possibly_damaging	24.6	1	0
13	97639218	C	T	c.796G>A	p.Glu266Lys	DAMAGING	probably_damaging	26.2	4	0
13	97639212	G	A	c.802C>T	p.Arg268Cys	DAMAGING	probably_damaging	31	1	0
13	97639211	C	T	c.803G>A	p.Arg268His	DAMAGING	probably_damaging	25.2	3	0
13	97639197	T	C	c.817A>G	p.Ser273Gly	DAMAGING	possibly_damaging	21.8	1	0
13	97639196	C	A	c.818G>T	p.Ser273Ile	DAMAGING	possibly_damaging	23.4	1	0
13	97639194	A	G	c.820T>C	p.Cys274Arg	DAMAGING	probably_damaging	24	1	0
13	97639193	C	A	c.821G>T	p.Cys274Phe	DAMAGING	probably_damaging	25	2	0
13	97639163	T	C	c.851A>G	p.Tyr284Cys	DAMAGING	probably_damaging	26.6	4	0
13	97639160	A	T	c.854T>A	p.Ile285Asn	TOLERATED	probably_damaging	26.9	1	0
13	97639148	G	C	c.866C>G	p.Pro289Arg	DAMAGING	probably_damaging	25	1	0
13	97639139	G	A	c.875C>T	p.Ala292Val	DAMAGING	benign	23.1	1	0
13	97639122	T	C	c.892A>G	p.Asn298Asp	DAMAGING	probably_damaging	26.2	1	0
13	97639120	G	T	c.894C>A	p.Asn298Lys	DAMAGING	probably_damaging	24.3	3	0
13	97639115	A	G	c.899T>C	p.Leu300Ser	DAMAGING	probably_damaging	22.4	1	0
13	97639081	C	A	c.933G>T	p.Gln311His	DAMAGING	benign	21.3	3	0

Supplementary Table S5. Summary of Urinary Risk Factors in *OXGR1* variant-associated individuals

Urinary Risk Factors	Frequency in *OXGR1* variant-associated families	Frequency in *OXGR1* variant-associated individuals
Hyperoxaluria	2/3 families	5/6
Hypocitraturia	1/2 families	4/5
Hypercalciuria	0/5 families	0/8

***Denominator is families or subjects where measured and data available**

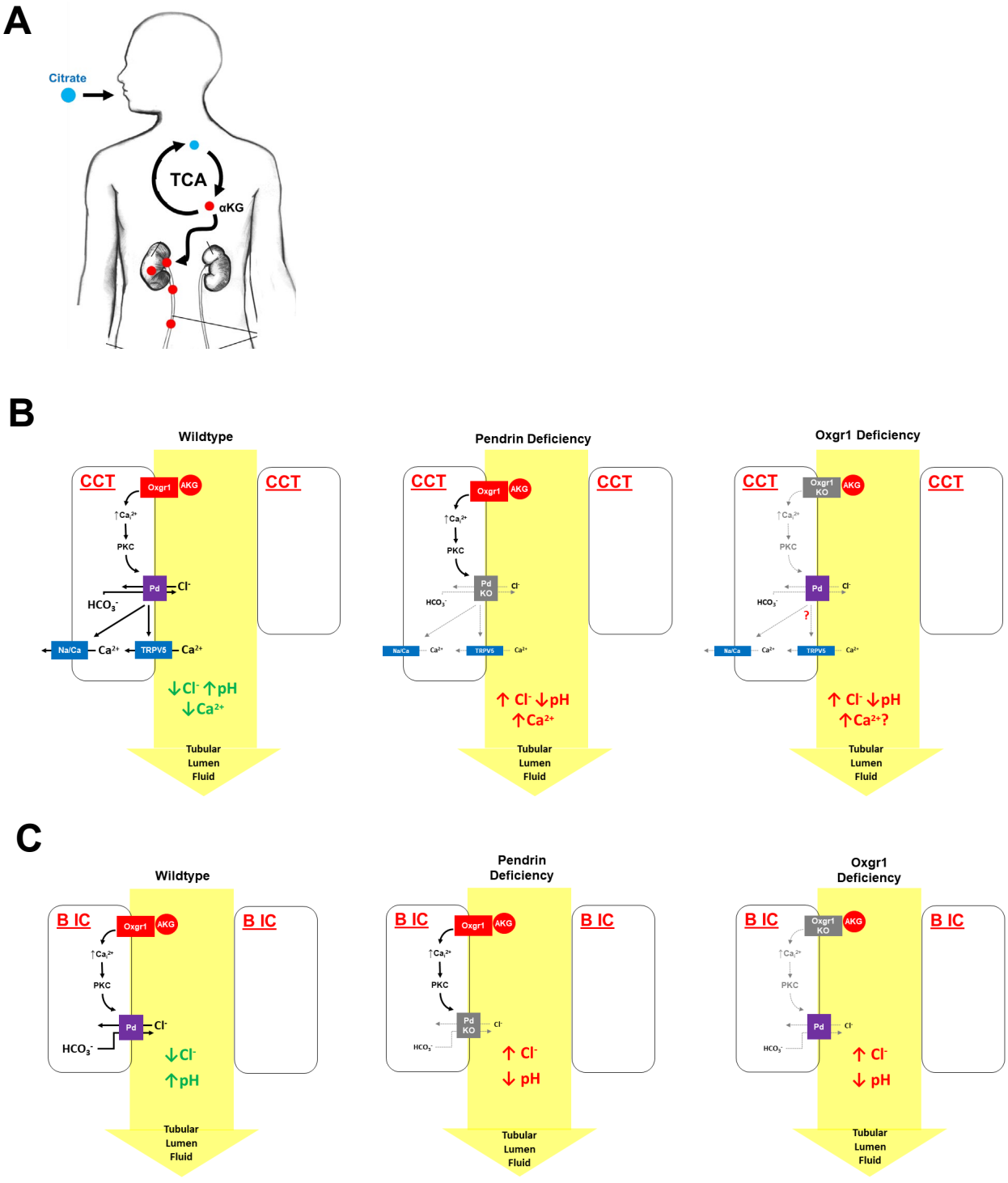
A
Citrate
TCA
αKG
B
Wildtype
CCT
Oxgr1
AKG
↑Ca2+
PKC
Pd
Cl-
HCO3-
Na/Ca
Ca2+
TRPV5
Ca2+
CCT
↓Cl- ↑pH
↓Ca2+
Tubular Lumen Fluid
Pendrin Deficiency
CCT
Oxgr1
AKG
↑Ca2+
PKC
Pd KO
Cl-
HCO3-
Na/Ca
Ca2+
TRPV5
Ca2+
CCT
↑ Cl- ↓pH
↑Ca2+
Tubular Lumen Fluid
Oxgr1 Deficiency
CCT
Oxgr1 KO
AKG
↑Ca2+
PKC
Pd
Cl-
HCO3-
?
Na/Ca
Ca2+
TRPV5
Ca2+
CCT
↑ Cl- ↓pH
↑Ca2+?
Tubular Lumen Fluid
C
Wildtype
B IC
Oxgr1
AKG
↑Ca2+
PKC
Pd
Cl-
HCO3-
B IC
↓Cl-
↑pH
Tubular Lumen Fluid
Pendrin Deficiency
B IC
Oxgr1
AKG
↑Ca2+
PKC
Pd KO
Cl-
HCO3-
B IC
↑ Cl-
↓ pH
Tubular Lumen Fluid
Oxgr1 Deficiency
B IC
Oxgr1 KO
AKG
↑Ca2+
PKC
Pd
Cl-
HCO3-
B IC
↑ Cl-
↓ pH
Tubular Lumen Fluid

Supplementary Figure 1. Mechanisms of OXGR1 signaling in renal epithelium.

(A) Citrate is metabolized into alpha-ketoglutarate (AKG) through the tri-carboxylic acid cycle (TCA) and excreted into the urine.

(B) Within the wildtype nephron in mice (left panel), Oxgr1 is expressed in cortical connecting tubule cells with Pendrin. Filtered AKG stimulates Oxgr1 activity that, through increased Ca^{2+} levels and Protein Kinase C (PKC), promotes Pendrin (Pd) activity. This leads to increased bicarbonate secretion into and chloride reabsorption from the tubular fluid. Pendrin also positively regulates the expression of apical Ca^{2+}channel TRPV5 and basolateral sodium-calcium exchanger (NCX1) to mediate transepithelial calcium transport. In Pendin KO mice (middle panel), Pendrin deficiency is associated with impaired urine alkalinization and increase chloride secretion in addition to calcium wasting associated with reduced expression of calcium transporters. Oxgr1 deficiency (right panel) phenocopies the effects of Pendrin deficiency on bicarbonate and chloride handling. It remains unknown if Oxgr1 deficiency similarly impairs calcium reabsorption.

(C) Within the wildtype nephron in mice (left panel), Oxgr1 is expressed in Type B intercalated cells with Pendrin. Filtered AKG stimulates Oxgr1 activity that, through increased Ca^{2+} levels and Protein Kinase C (PKC), promotes Pendrin (Pd) activity. This leads to increased bicarbonate secretion into and chloride reabsorption from the tubular fluid. In Pendrin KO mice (middle panel), Pendrin deficiency is associated with impaired urine alkalinization and increase chloride secretion. Oxgr1 deficiency (right panel) phenocopies the effects of Pendrin deficiency on bicarbonate and chloride handling.

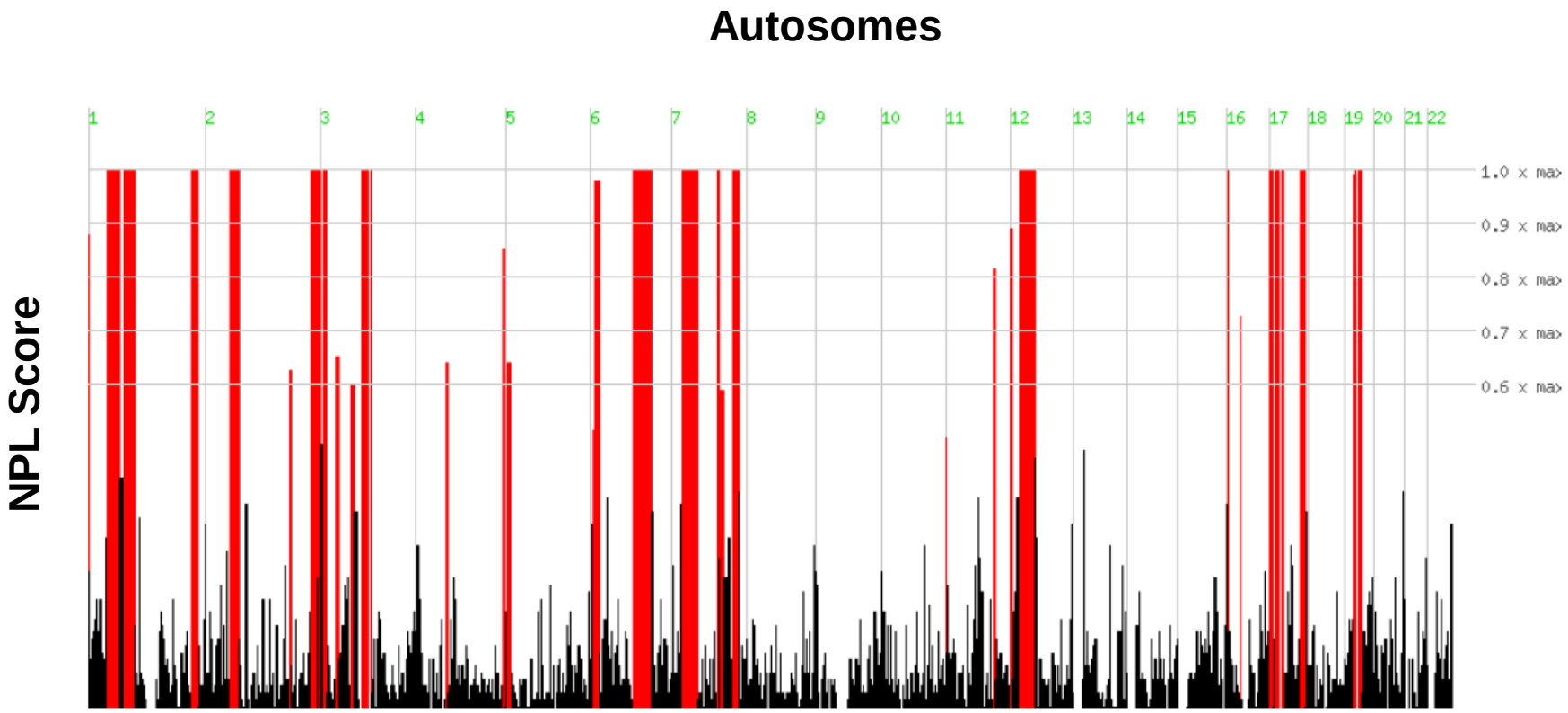

Figure S2. Homozygosity Mapping based on exome variants for B1467_22
Homozygosity mapping was performed by mapping profiles of nonparametric lod (NPL) scores across the genome based on WES variant data using Homozygosity Mapper.

A.

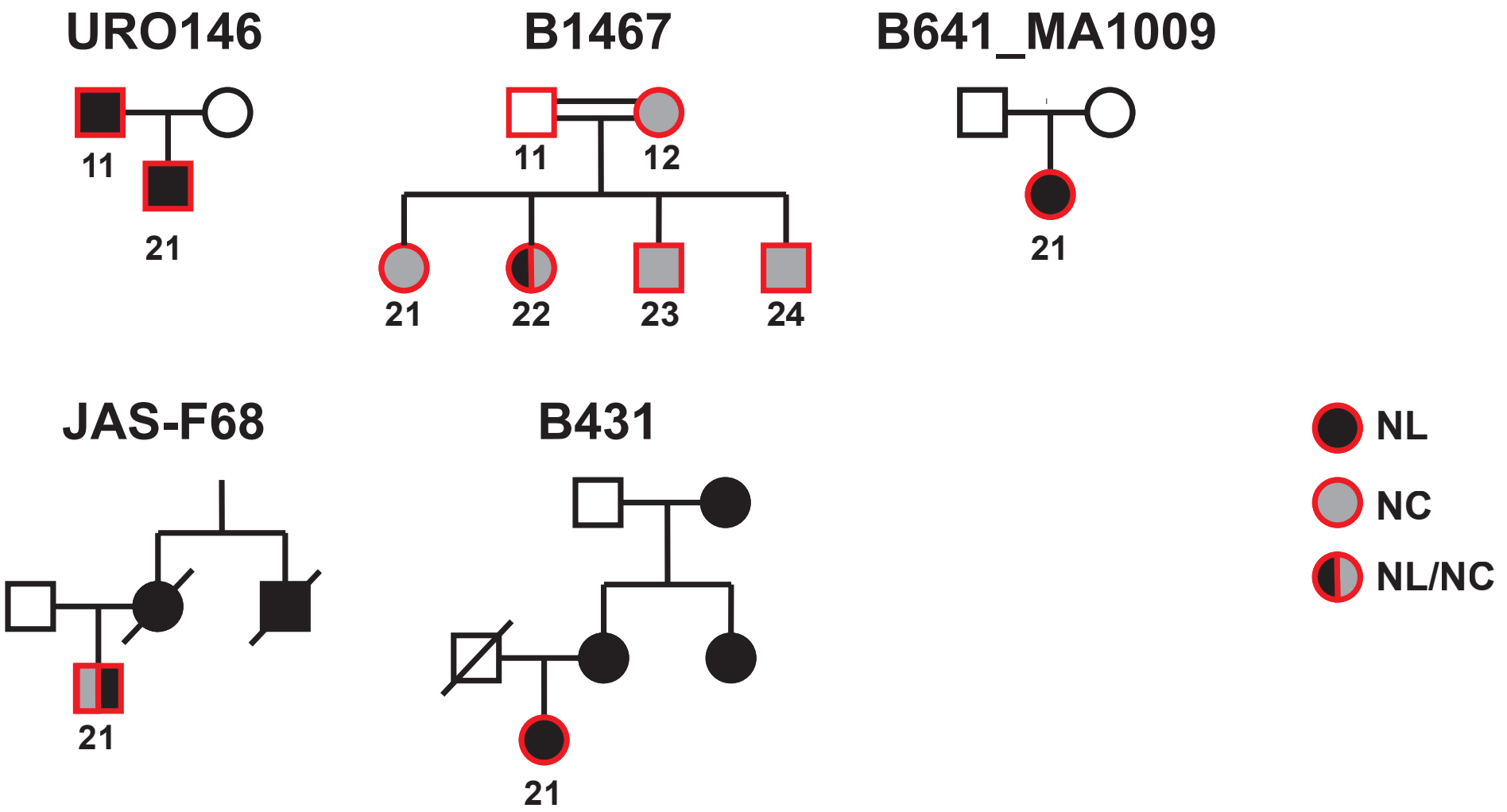

B.

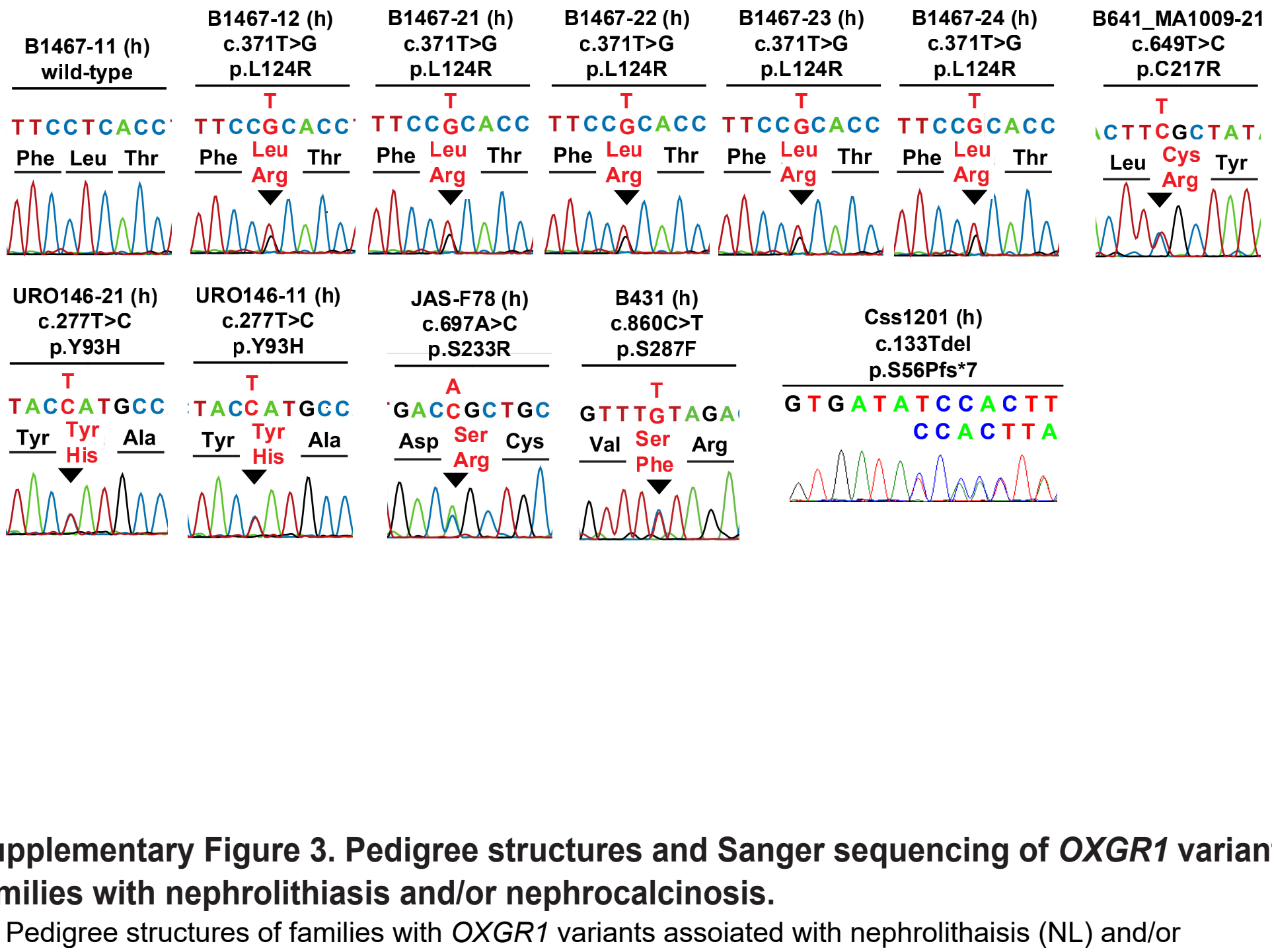

Supplementary Figure 3. Pedigree structures and Sanger sequencing of *OXGR1* variants in families with nephrolithiasis and/or nephrocalcinosis.

(A) Pedigree structures of families with *OXGR1* variants assoiated with nephrolithaisis (NL) and/or nephrocalcinosis (NC). A legend at the bottom right defines the phenotype associated with each shading. Subjects for whom DNA was available are circled in red.

(B) Sanger sequencing of *OXGR1* variants in families with NL and/or NC are shown.

A

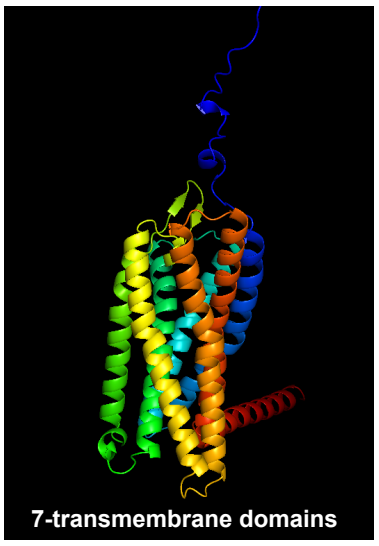

B

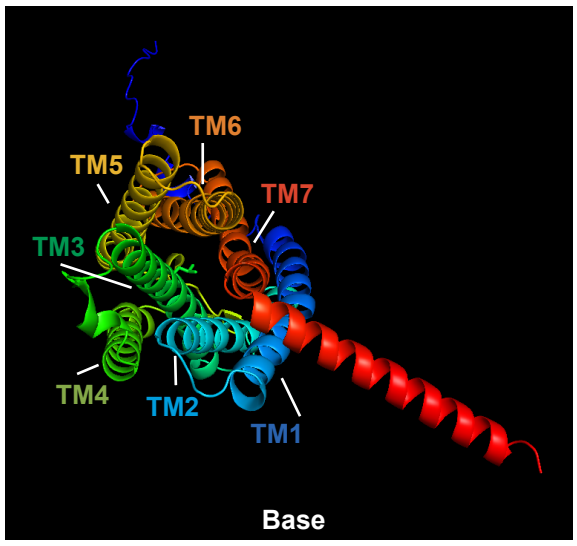

C

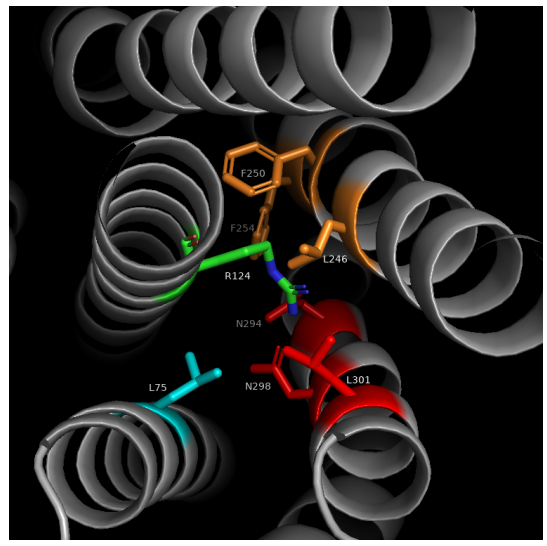

D

		OXGR1 Transmembrane Domain 3 Amino Acid Sequence																													
		D	F	M	C	K	F	I	R	F	S	F	H	F	N	L	Y	S	S	I	L	L	F	T	D	E	N	I	P	L
Amino Acid Frequency	H	14	9	5	1	6	0	11	11	1	0	7	10	1	2	0	11	3	1	0	1	21	1	0	1	0	1	0	9	3	12
	K	13	3	0	0	106	0	2	6	0	0	6	7	0	1	2	0	0	0	0	1	1	0	0	0	0	0	0	0	3	0
	R	22	6	1	4	56	0	12	15	0	0	5	3	0	0	11	1	0	0	0	0	0	0	0	0	0	0	0	1	282	2
	D	44	1	0	6	19	0	1	5	1	0	58	8	0	0	0	0	0	1	0	0	0	0	0	0	0	0	0	192	0	0
	E	25	7	0	0	8	0	5	8	0	0	4	8	2	0	0	10	2	5	0	3	0	0	0	1	0	0	0	64	0	0
	N	15	3	0	0	14	0	4	14	0	0	1	3	1	77	2	8	2	0	4	4	28	1	1	0	0	3	0	9	0	0
	Q	14	1	3	1	16	0	5	8	0	1	25	5	0	1	5	7	0	1	0	1	1	0	0	0	0	0	1	6	6	1
	S	27	9	9	4	9	5	26	31	36	10	8	21	12	63	26	23	48	215	7	15	47	1	18	9	0	167	3	1	0	5
	T	21	20	10	1	14	13	19	34	14	12	10	29	28	15	16	41	28	21	21	2	42	6	90	7	4	27	8	5	1	0
	A	20	43	23	0	6	28	12	29	40	16	9	14	21	25	7	10	112	10	17	14	4	3	45	107	4	89	19	2	0	2
	F	5	38	28	0	1	43	26	9	73	35	43	31	36	31	27	50	0	0	2	86	63	3	8	17	3	0	17	5	1	30
	I	3	19	21	0	2	42	25	13	7	40	18	14	27	1	13	11	12	0	117	10	14	30	7	12	168	0	65	0	0	0
	L	8	41	93	0	13	87	36	31	18	111	25	21	64	21	42	28	10	1	34	89	55	216	39	41	52	1	68	0	1	1
	M	1	1	29	0	1	8	7	7	4	17	21	6	27	4	54	1	2	0	17	11	12	14	6	3	40	0	2	0	0	2
	V	8	42	15	1	5	63	59	14	18	41	18	46	56	5	31	6	43	0	74	8	3	19	25	44	29	1	101	2	0	2
	W	3	4	5	0	1	2	25	0	2	0	1	2	1	1	1	0	0	0	0	10	0	0	0	2	0	0	3	0	0	11
	Y	7	9	4	1	3	3	15	8	39	1	24	48	6	2	13	80	0	0	0	23	0	1	0	1	0	0	8	0	1	197
	C	2	0	1	265	1	1	6	0	10	8	2	7	12	24	31	1	15	5	4	14	7	0	48	47	0	5	1	0	2	34
	G	15	17	33	1	2	4	1	40	31	4	11	15	6	22	17	11	23	36	3	8	2	4	10	7	0	5	3	4	0	1
	P	15	11	6	2	5	0	1	15	4	2	4	2	0	5	2	1	0	4	0	0	0	1	3	1	0	0	0	0	0	0
	Blank	18	16	14	13	12	1	2	2	2	2	0	0	0	0	0	0	0	0	0	0	0	0	0	0	0	1	1	0	0	0
	Total	300	300	300	300	300	300	300	300	300	300	300	300	300	300	300	300	300	300	300	300	300	300	300	300	300	300	300	300	300	300

L124R

E

M	N	E	P	L	D	Y	L	A	N	A	S	D	F	P	D	Y	A	A	A	F	G	N	C	T	D	E	N	I	P	L	K	M	H	Y	L	P	V	I	Y	G	I	I	F	L	V	G	F	P	G
12	0	0	1	0	2	0	0	0	8	0	5	0	0	7	0	0	5	5	0	1	1	3	63	1	10	3	10	5	26	28	16	5	6	5	75	65	61	32	109	41	40	84	105	96	98	164	21	27	206

N	A	V	V	I	S	T	Y	I	F	K	M	R	P	W	K	S	S	T	I	I	M	L	N	L	A	C	T	D	L	L	Y	L	T	S	L	P	F	L	I	H	Y	Y	A	S	G	E	N	W	I
294	45	34	196	78	6	20	5	22	28	8	18	68	11	12	29	58	28	24	73	11	23	96	152	272	220	19	28	276	174	189	19	57	14	29	115	204	106	20	59	13	50	71	50	18	35	13	15	218	21

F	G	D	F	M	C	K	F	I	R	F	S	F	H	F	N	L	Y	S	S	I	L	F	L	T	C	F	S	I	F	R	Y	C	V	I	I	H	P	M	S	C	F	S	I	H	K	T	R	C	A
140	183	44	38	29	265	106	43	25	15	73	10	43	10	36	77	42	80	48	215	117	89	63	216	90	47	3	167	65	5	282	197	7	20	138	13	95	204	22	22	5	8	5	20	3	17	16	81	11	154

V	V	A	C	A	V	V	W	I	I	S	L	V	A	V	I	P	M	T	F	L	I	T	S	T	N	R	T	N	R	S	A	C	L	D	L	T	S	S	D	E	L	N	T	I	K	W	Y	N	L
29	58	34	59	70	37	91	287	40	33	118	89	41	32	12	45	180	10	11	40	30	6	26	17	16	9	10	8	17	18	20	25	247	23	17	32	11	34	12	12	25	34	8	7	4	21	7	97	15	70

I	L	T	A	T	T	F	C	L	P	L	V	I	V	T	L	C	Y	T	T	I	I	H	T	L	T	H	G	L	Q	T	D	S	C	L	K	Q	K	A	R	R	L	T	I	L	L	L	A	F
28	64	28	22	18	14	201	12	100	221	135	36	95	27	25	43	122	221	31	6	168	45	12	46	144	7	9	9	17	21	9	5	20	6	7	34	16	128	95	2	86	53	11	22	38	45	68	68	61	239

Y	V	C	F	L	P	F	H	I	L	R	V	I	R	I	E	S	R	L	L	S	I	S	C	S	I	E	N	Q	I	H	E	A	Y	I	V	S	R	P	L	A	A	L	N	T	F	G	N	L	L
5	80	209	47	111	290	89	78	86	52	11	1	4	20	14	2	24	25	33	9	6	2	20	62	13	6	24	15	8	24	13	11	57	46	20	75	45	19	6	188	115	16	79	196	19	9	1	213	2	61

L	Y	V	V	V	S	D	N	F	Q	Q	A	V	C	S	T	V	R	C	K	V	S	G	N	L	E	Q	A	K	K	I	S	Y	S	N	N	P
101	266	27	10	46	71	14	39	194	41	22	62	23	9	26	13	21	36	65	16	10	21	13	6	12	6	2	6	10	5	2	2	1	3	2	3	6	

Supplementary Figure 4. Structural modeling and paralog analysis of amino acids impacted by *OXGR1* variants.

(A) Ribbon structure of human OXGR1 receptor portrayed from side of seven transmembrane (TM) domains.

(B) Predicted human OXGR1 structure shown as in (A) from base.

(C) The L124R variant is modeled on the predicted human OXGR1 receptor structure and results in a larger polar arginine residue protruding into this pocket.

(D) Multiple sequence alignment (MSA) of the primary amino acid sequences of OXGR1 and 300 additional G-protein coupled receptors (GPCRs) obtained from GPCR Sarfari (ChEMBL). The conservation of amino acids is shown via a frequency table, where the primary amino acid sequence of TM3 of OXGR1 is shown in the first row. The absolute frequency of amino acids aligned with each OXGR1 amino acid in the MSA is shown below. Leucine 124 (black arrow) is conserved in 216 of 300 GPCRs (72%), while arginine, predicted to result from case variant c.371T>G, is not observed in any GPCRs at this position. Red shading indicates conservation in >2/3 of GPCRs. Orange highlighting indicates conservation across 1/3 to 2/3 of GPCRs.

(E) Frequency diagram shows the conservation of each amino acid in OXGR1 across 300 other GPCRs by MSA. Colored bars represent transmembrane domains. Leucine 124, predicted to be mutated by patient variant c.371T>G, is conserved in 216 of 300 GPCRs (72%). Cysteine 217, predicted to be mutated by patient variant c.649T>C, is conserved in 122 of 300 GPCRs. No other amino acids, predicted to be mutated by *OXGR1* case variants, are conserved in more than 1/3 of GPCRs.

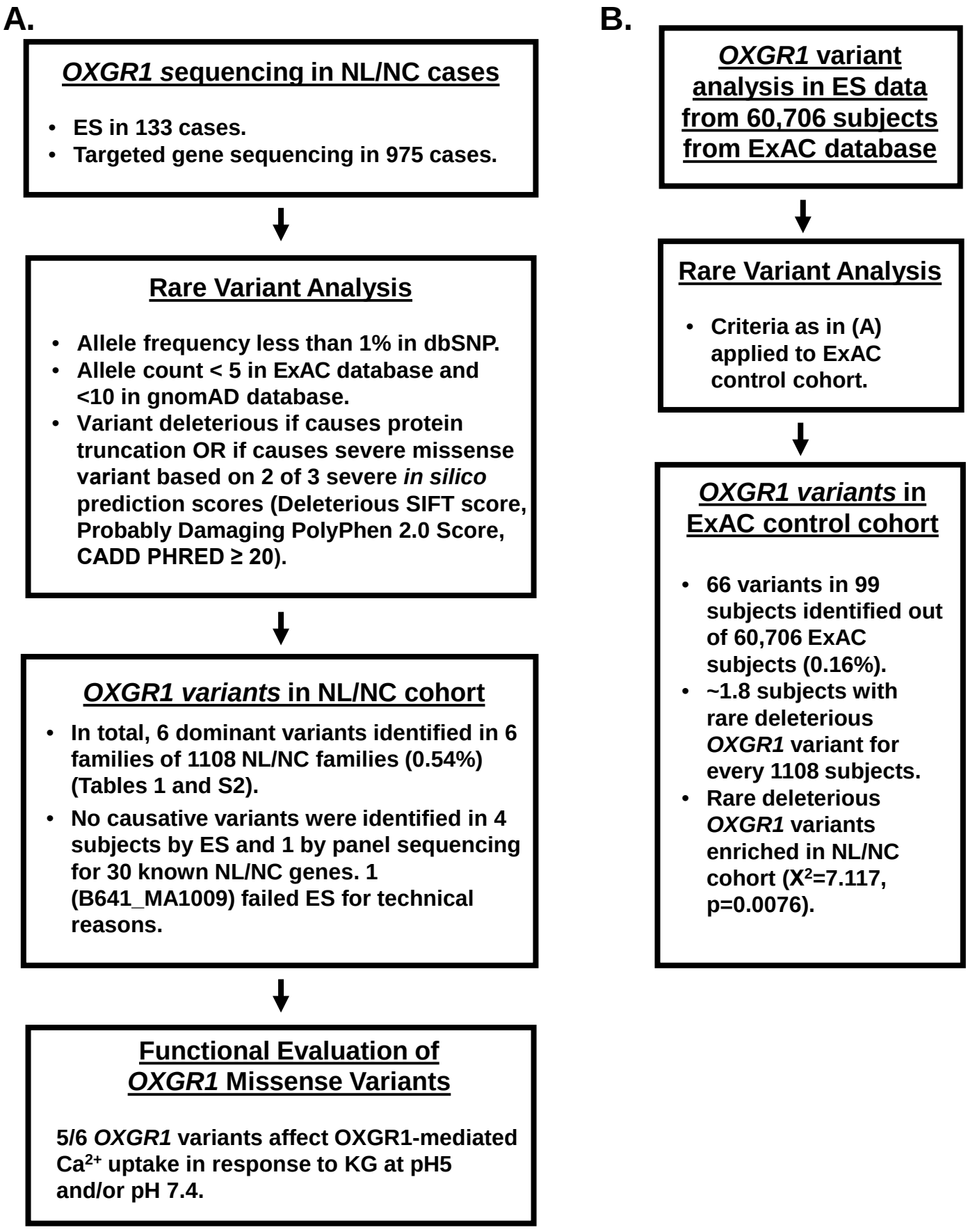
A.
OXGR1 sequencing in NL/NC cases
• ES in 133 cases.
• Targeted gene sequencing in 975 cases.
Rare Variant Analysis
• Allele frequency less than 1% in dbSNP.
• Allele count < 5 in ExAC database and <10 in gnomAD database.
• Variant deleterious if causes protein truncation OR if causes severe missense variant based on 2 of 3 severe in silico prediction scores (Deleterious SIFT score, Probably Damaging PolyPhen 2.0 Score, CADD PHRED ≥ 20).
OXGR1 variants in NL/NC cohort
• In total, 6 dominant variants identified in 6 families of 1108 NL/NC families (0.54%) (Tables 1 and S2).
• No causative variants were identified in 4 subjects by ES and 1 by panel sequencing for 30 known NL/NC genes. 1 (B641_MA1009) failed ES for technical reasons.
Functional Evaluation of OXGR1 Missense Variants
5/6 OXGR1 variants affect OXGR1-mediated Ca2+ uptake in response to KG at pH5 and/or pH 7.4.
B.
OXGR1 variant analysis in ES data from 60,706 subjects from ExAC database
Rare Variant Analysis
• Criteria as in (A) applied to ExAC control cohort.
OXGR1 variants in ExAC control cohort
• 66 variants in 99 subjects identified out of 60,706 ExAC subjects (0.16%).
• ~1.8 subjects with rare deleterious OXGR1 variant for every 1108 subjects.
• Rare deleterious OXGR1 variants enriched in NL/NC cohort (X2=7.117, p=0.0076).

Supplementary Figure 5. Sequencing and variant interpretation for *OXGR1* locus in 1108 subjects with nephrolithiasis (NL) and/or nephrocalcinosis (NC) and in the ExAC cohort.

(A) DNA samples from 133 NL/NC subjects were evaluated by exome sequencing (ES), and 975 NL/NC subjects were evaluated by targeted amplification of the *OXGR1* locus. Variants were filtered, yielding 5 additional variants in 5 families with NL/NC. These subjects were also evaluated for variants in known NL/NC disease genes as shown. All missense variants were functionally assessed for impact on alpha-ketoglutarate (KG)-dependent Ca2+ influx in *Xenopus* oocytes, demonstrating a functional alteration in 5 of 6 variants.

(B) ES data from 60,706 ExAC database subjects was interrogated for *OXGR1* variants as described in (A). 66 variants in 99 subjects were identified (0.16%). Assuming no subjects have multiple rare variants, this equates to ~1.8 subjects with an *OXGR1* variant per 1108 subjects. Rare deleterious *OXGR1* variants are enriched in the NL/NC cohort (X^2=7.117, p=0.0076).

A

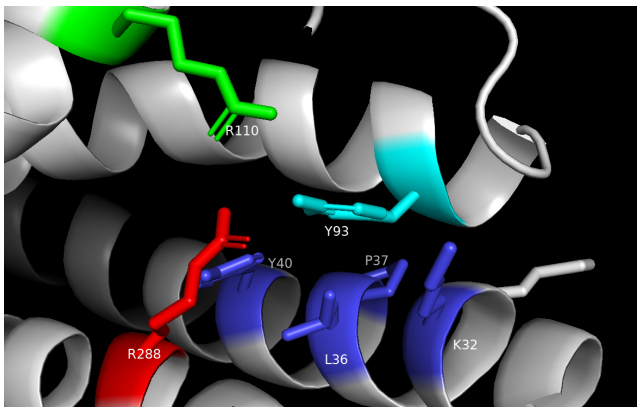

B

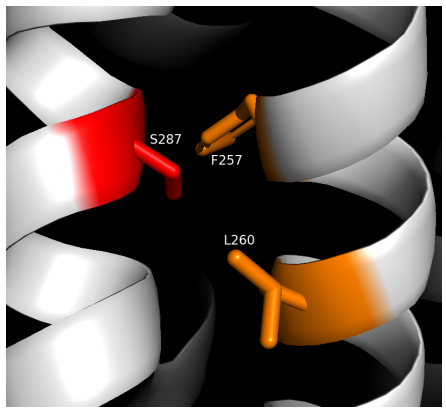

C

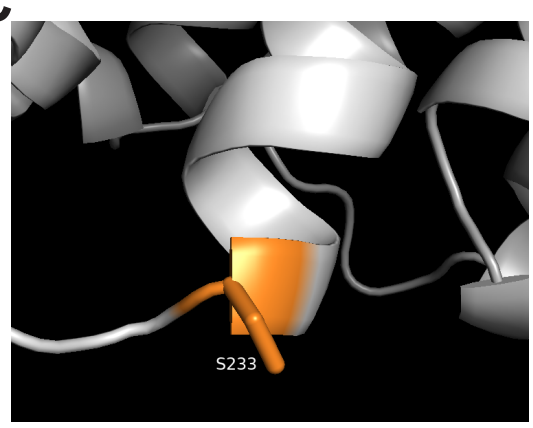

D

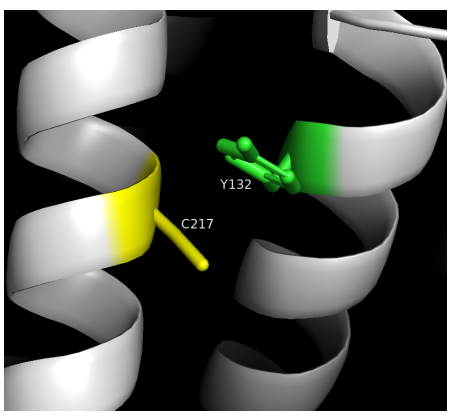

E

OXGR1 Variant	Site Directed Mutator Predicted pseudo ΔΔG Using OXGR1 structure AF-Q96P68-F1	Stability Outcome
L124R	-2.7	Reduced Stability
Y93H	-1.42	Reduced Stability
C217R	-0.73	Reduced Stability
S233R	1.07	Increased Stability
S287F	0.44	Increased Stability

Supplementary Figure 6. Structural modeling and analysis of NL/NC-associated OXGR1 variants.

(A) Position of Y93 and adjacent amino acid residues is portrayed on human OXGR1 (AF-Q96P68-F1-model_v2). It is within 4 angstroms of six other residues, four of which are also polar.

(B) S287 is shown and is within 4 angstroms of other polar amino acid residues.

(C) S233 is shown and is not within 4 angstroms of other polar amino acid residues.

(D) C217 is shown and is not within 4 angstroms of other cysteine residues.

(E) Site Directed Mutator was employed to predict thermodynamic instability caused by *OXGR1* NL/NC-associated variant using the human OXGR1 structure AF-Q96P68-F1-model_v2.

A

337 AA protein
NP_001333123

NBP2-42169

B

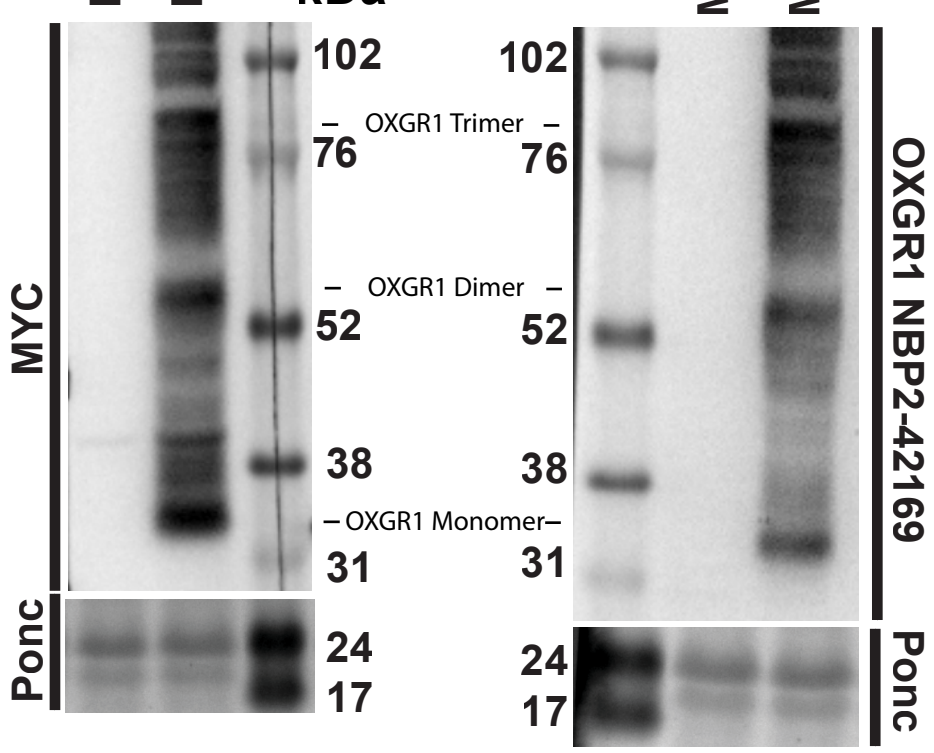

C

D

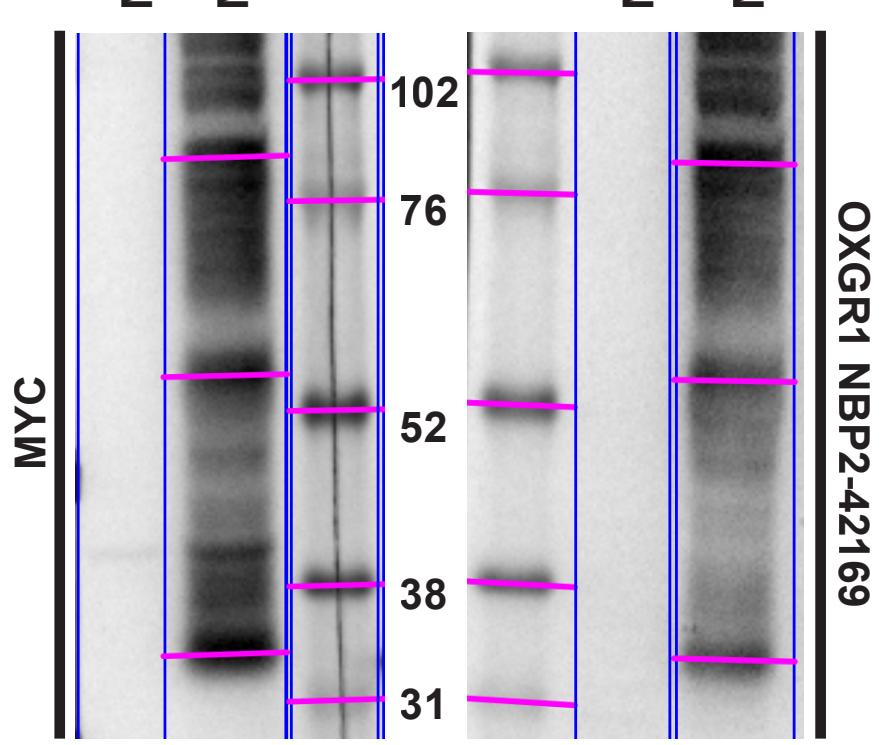

E

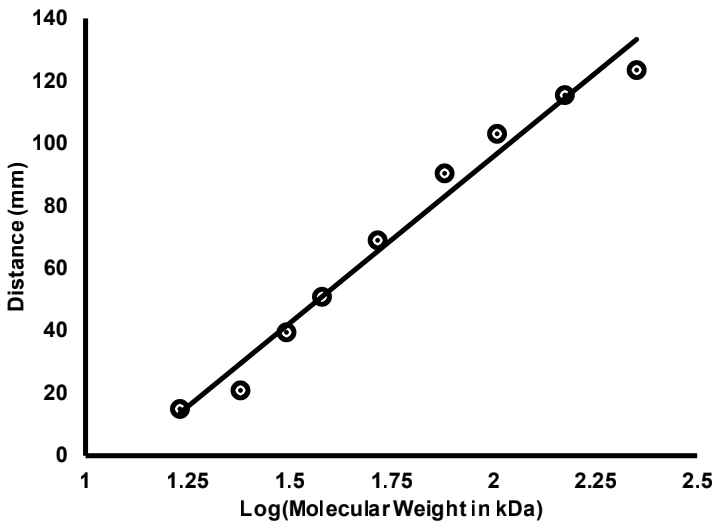

F

Antibody	Band	Distance (mm)	MW (kDA)	Ratio
MYC	1	53	32.5	1.0
	2	81.5	60.4	1.9
	3	104	98.7	3.0
OXGR1	1	54.5	32.5	1.0
	2	82.5	60.1	1.8
	3	104	96.4	3.0

G

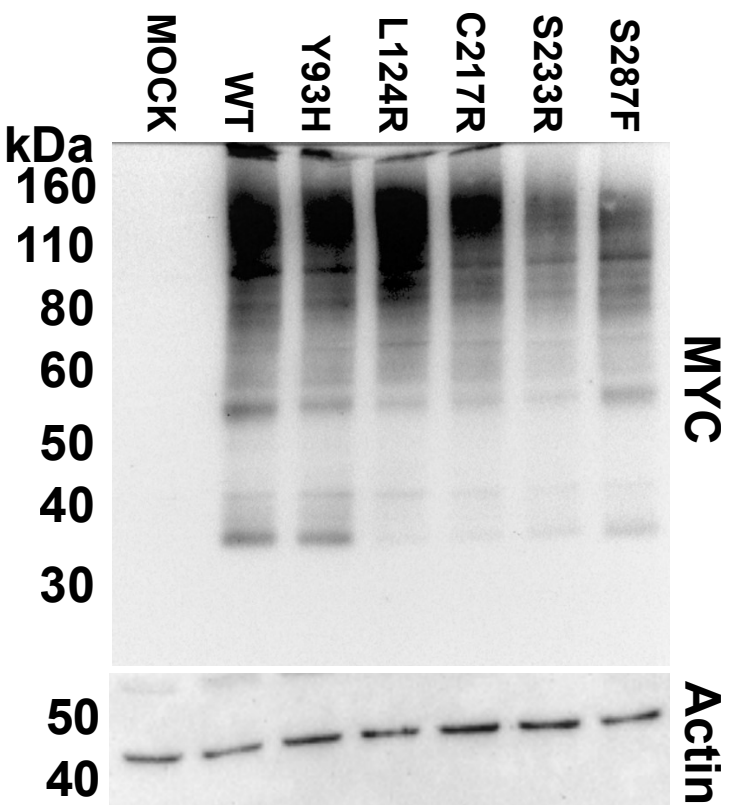

H

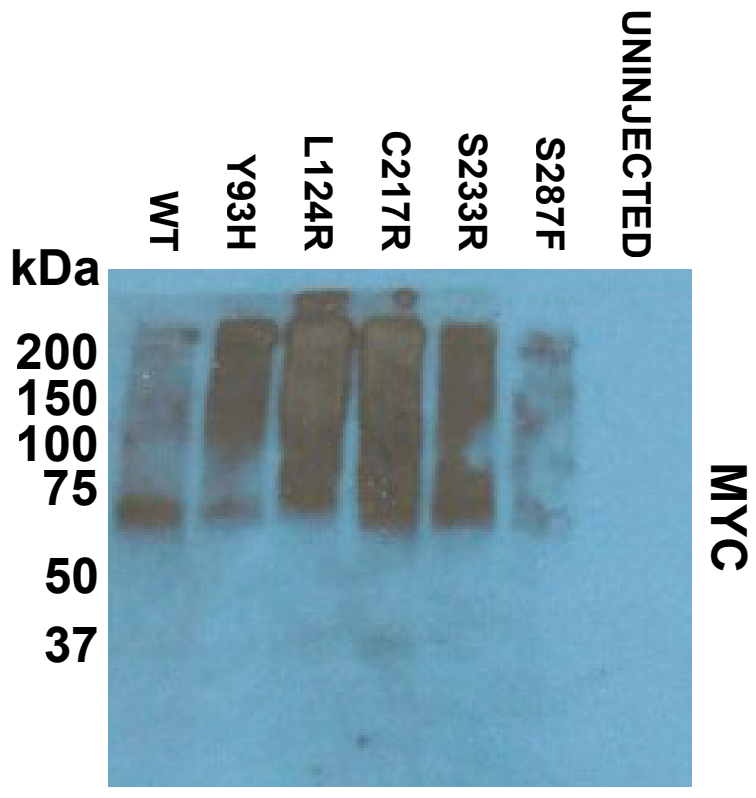

Supplementary Figure 7. *OXGR1* cDNA expression results in multimeric banding pattern in HEK293T cell lines and in *Xenopus* oocytes that is not affected by NL/NC variants.

(A) Diagram of human OXGR1 protein showing immunogen region for OXGR1 antibody NBP2-42169.

(B) Anti-MYC tag and (C) anti-OXGR1 immunoblots of clarified lysates from HEK293T cells transfected with mock MYC plasmid (MOCK) or N-terminal MYC-tagged wildtype OXGR1 are shown. ~35 kDa monomeric OXGR1 was detected as well as OXGR1 oligomers.

(D) The bands of the protein standard ladder and major OXGR1 oligomer bands from immunblotting are overlayed with lines used to generate standard curve of molecular weight versus distance from the 10 kDA marker on protein ladder.

(E) Plot of logarithm of molecular weights of ladder protein standards relative to distance from bottom marker (10 kDA) is shown with trendline.

(F) Based on linear equation of trendline (E), estimated molecular weights of major OXGR1 oligomeric bands from anti-MYC and anti-OXGR1 immunoblotting in (D). These correspond to OXGR1 monomers, dimers and trimers.

(G) Anti-MYC tag immunoblot of clarified lysates from HEK293T cells transfected with mock MYC plasmid (MOCK), N-terminal MYC-tagged wildtype OXGR1, or tagged constructs bearing NL/NC patient derived variants is shown.

(H) Anti-MYC tag immunoblot of clarified lysates from whole uninjected oocytes or from oocytes injected 48-72h previously with 50 ng cRNA encoding myc-tagged wild type OXGR1 or the indicated OXGR1 variants.

A

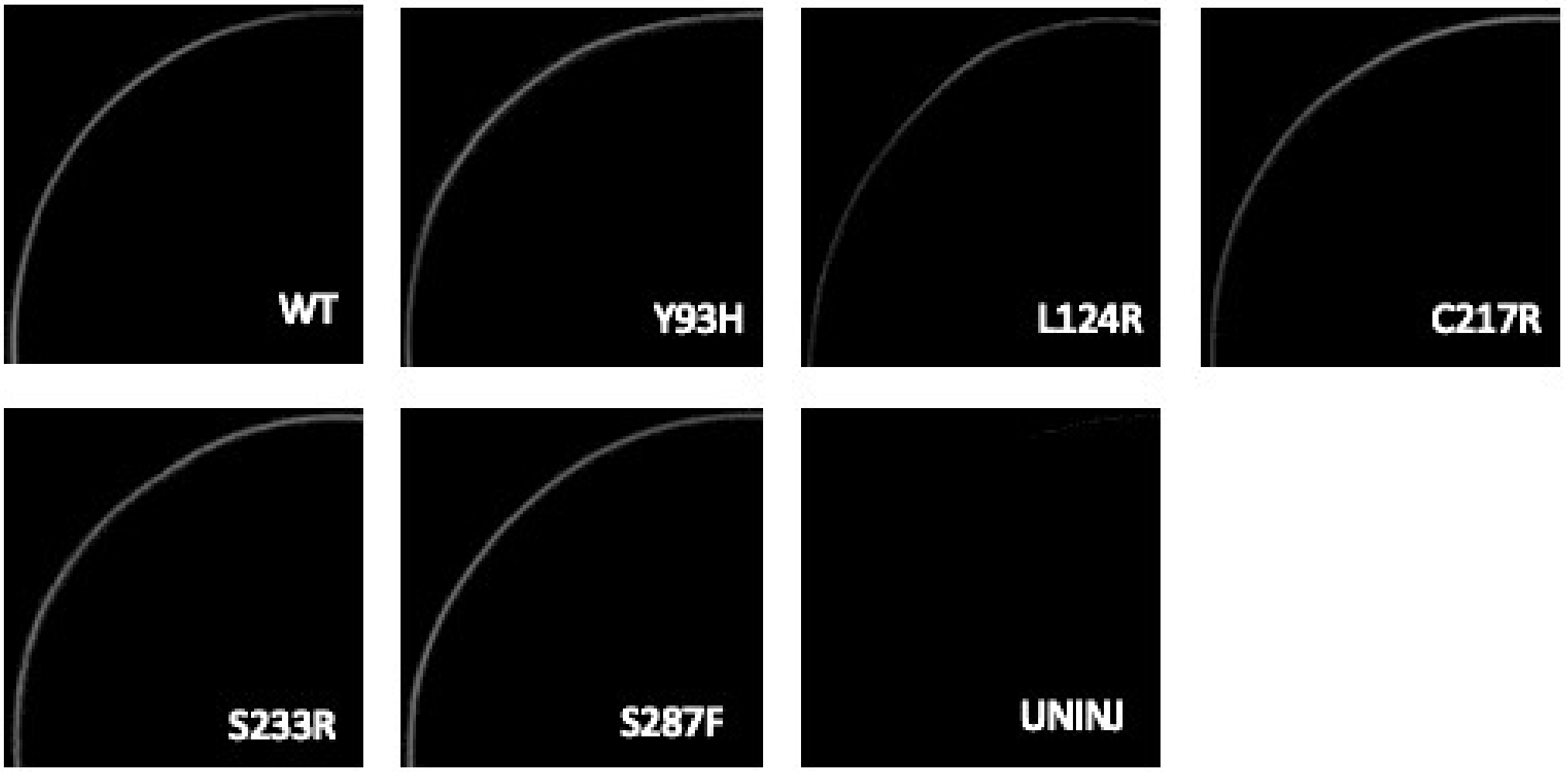
WT
Y93H
L124R
C217R
S233R
S287F
UNINJ

B

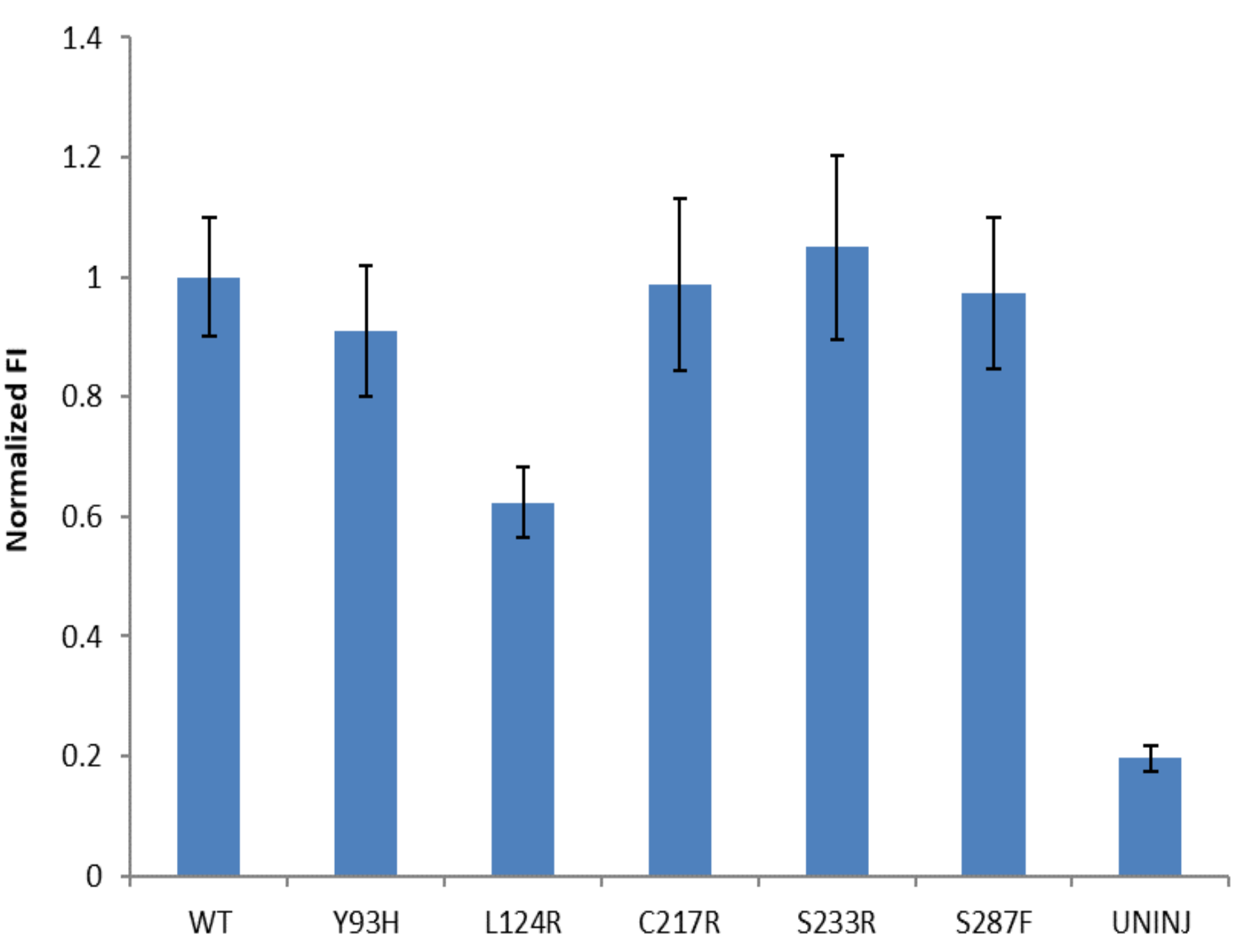
Normalized FI
1.4
1.2
1
0.8
0.6
0.4
0.2
0
WT
Y93H
L124R
C217R
S233R
S287F
UNINJ

Supplementary Figure 8. *OXGR1* cRNA expression results in expected expression at or near the surface of *Xenopus* oocytes that is not affected by NL/NC variants.

(A) Equatorial plane confocal sections of whole mount anti-MYC immunofluorescence micrographs of representative uninjected oocytes and oocytes injected 48-72 h previously with cRNA (50 ng) encoding C-terminal myc-tagged wild type OXGR1 or the indicated variants.

(B) Histogram of immunofluorescence signal from (A) is displayed.

A.

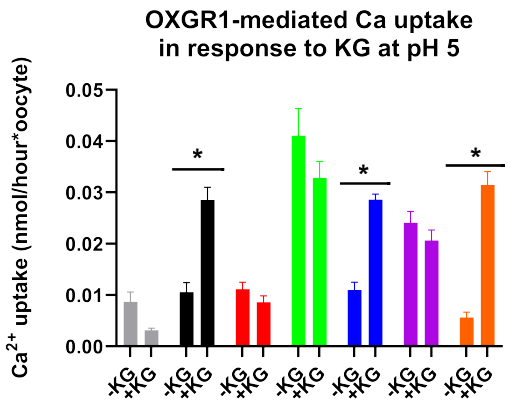
OXGR1-mediated Ca uptake
in response to KG at pH 5
Ca2+ uptake (nmol/hour*oocyte)
0.05
0.04
0.03
0.02
0.01
0.00
*
*
*
-KG
+KG

B.

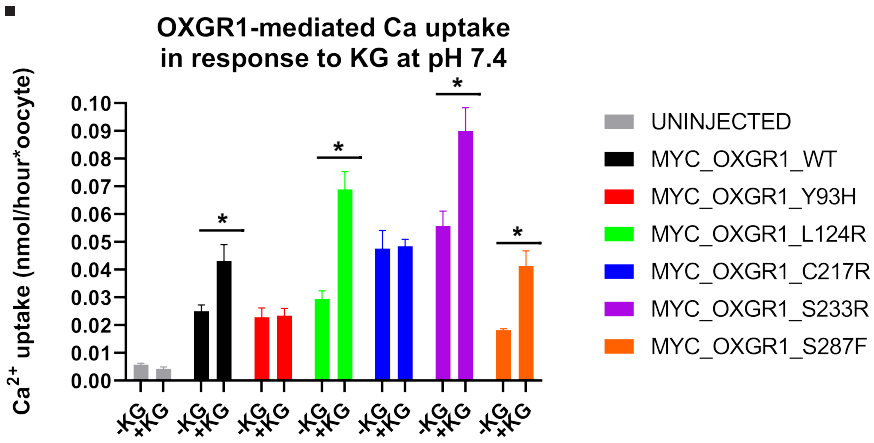
OXGR1-mediated Ca uptake
in response to KG at pH 7.4
Ca2+ uptake (nmol/hour*oocyte)
0.10
0.09
0.08
0.07
0.06
0.05
0.04
0.03
0.02
0.01
0.00
*
*
*
*
-KG
+KG
UNINJECTED
MYC_OXGR1_WT
MYC_OXGR1_Y93H
MYC_OXGR1_L124R
MYC_OXGR1_C217R
MYC_OXGR1_S233R
MYC_OXGR1_S287F

Supplementary Figure 9. OXGR1-mediated alpha-ketoglutarate dependent Ca^{2+} uptake in *Xenopus* oocytes.

(A) Ca^{2+} uptake into *Xenopus* oocytes injected 48-72 hours previously with water or with cRNA (40 ng) encoding wild type human OXGR1 or the indicated variants. Uptake was measured at bath pH 5.0 for 30 min in the absence (-KG) or presence (+KG) of bath alpha-ketoglutarate (1 mM). *p<0.05 by Student's *t*-test.

(B) Ca^{2+} uptake into *Xenopus* oocytes injected 48-72 h previously with water or with cRNA (25 ng) was measured at bath pH 7.4 for 30 min in absence (-KG) or presence (+KG) of bath alpha-ketoglutarate (1 mM). *p<0.05 by Student's *t*-test.